Physica Medica 59 (2019) 37–46

Contents lists available at ScienceDirect

Physica Medica

journal homepage: www.elsevier.com/locate/ejmp

Original paper

EPID sensitivity to delivery errors for pre-treatment verification of lung SBRT VMAT plans

Thahabah Alharthi[a,b,c,d,*], Sankar Arumugam[c,e], Phil Vial[c,d,e], Lois Holloway[a,c,d,e,f], David Thwaites[a]

[a] Institute of Medical Physics, School of Physics, The University of Sydney, Sydney, New South Wales, Australia
[b] School of Medicine, Taif University, Taif, Saudi Arabia
[c] Liverpool and Macarthur Cancer Therapy Centers, Liverpool, NSW, Australia
[d] Ingham Institute for Applied Medical Research, Sydney, NSW, Australia
[e] South Western Sydney Clinical School, University of New South Wales, Sydney, NSW, Australia
[f] Centre for Medical Radiation Physics, University of Wollongong, Wollongong, NSW, Australia

ARTICLE INFO

Keywords:
Lung SBRT VMAT
Delivery error
EPID

ABSTRACT

Purpose: To study the sensitivity of an Electronic Portal Imaging Device (EPID) in detecting delivery errors for VMAT lung stereotactic body radiotherapy (SBRT) using the Collapsed Arc method.
Methods: Baseline VMAT plans and plans with errors intentionally introduced were generated for 15 lung SBRT patients. Three types of errors were introduced by modifying collimator angles and multi-leaf collimator (MLC) field sizes (MLCFS) and MLC shifts by ± 5, ± 2, and ± 1° or millimeters. A total of 103 plans were measured with EPID on an Elekta Synergy Linear Accelerator (Agility MLC) and compared to both the original treatment planning system (TPS) Collapsed Arc dose matrix and the no-error plan baseline EPID measurements. Gamma analysis was performed using the OmniPro-I'mRT (IBA Dosimetry) software and gamma criteria of 1%/1 mm, 2%/1 mm, 2%/2 mm, and 3%/3.
Results: When the error-introduced EPID measured dose matrices were compared to the TPS matrices, the majority of simulated errors were detected with gamma tolerance of 2%/1 mm and 1%/1 mm. When the error-introduced EPID measured dose matrices were compared to the baseline EPID measurements, all the MLCFS and MLC shift errors, and ± 5°collimator errors were detected using 2%/1 mm and 1%/1 mm gamma criteria.
Conclusion: This work demonstrates the feasibility and effectiveness of the collapsed arc technique and EPID for pre-treatment verification of lung SBRT VMAT plans. The EPID was able to detect the majority of MLC and the larger collimator errors with sensitivity to errors depending on the gamma tolerances.

1. Introduction

Radiation therapy delivery has become more complex with the introduction of volumetric modulated arc therapy (VMAT) using continuously modulated multi-leaf collimator (MLC) positions as well as gantry speed rotation and dose-rate [1,2]. Moreover, along with the current advances in radiotherapy techniques, interest in dose escalation and the use of hypofractionated stereotactic body radiotherapy (SBRT) has been growing [3–5]. SBRT involves the delivery of substantially larger doses per fraction over fewer fractions compared to conventional radiotherapy. Dosimetry verification and patient-specific quality assurance (QA) tests are particularly important in such a complex treatment to ensure accurate treatment delivery [6,7]. For conventionally fractionated VMAT pretreatment QA, many commercial solutions have been used including ionization chambers [8], film dosimetry [4], two-dimensional (2D) array detectors such as OCTAVIUS, MatriXX/COMPASS system, and electronic portal imaging device (EPID) [9,10], semi 3D dosimetric systems [11,12] and gel dosimetry [13]. Some of these detectors are often time-consuming to set up or have a relatively low spatial resolution. Electronic portal imaging devices (EPID) have been used for dosimetric verification including patient-specific VMAT verification [14–17]. EPIDs are available on all commercial linear accelerators and represent an efficient dosimeter due to high resolution and reproducibility, easy setup, immediate digital format and large sensitive area [18]. Several studies have investigated different applications of using the EPID as a patient dosimeter including; pretreatment verification for either fixed or rotating gantry [18–20], in vivo dosimetry, and full 3D dose estimation of the patient treatment [16,21,22]. The

* Corresponding author.
E-mail address: talh5880@uni.sydney.edu.au (T. Alharthi).

https://doi.org/10.1016/j.ejmp.2019.02.007
Received 12 December 2018; Received in revised form 31 January 2019; Accepted 10 February 2019
Available online 26 February 2019

potential of using EPID for detecting various delivery errors has been well demonstrated in previous studies [23–25]. Previous studies have also shown that different dosimetry systems exhibit different ability to detect dosimetric errors arising from uncertainties introduced into baseline plans [26,27,28]. The detector resolution and gamma criteria have a significant impact on the pre-treatment verification and error detection as demonstrated by Bruschi et al. [26] and Woon et al. [27]. This places an emphasis on the need to perform an accurate dose verification for each detector with respect to its resolution particularly for SBRT QA in which the impact of each fraction is large. For hypofractionated lung SBRT VMAT pretreatment QA, different groups have utilized various methods and dosimetric systems to verify treatment plans such as ArcCHECK [29–32], Leuco crystal violet (LCV) micelle gel [33], MapCHECK and EBT2 films [28,33], machine log file [34], and EPID-based in vivo dosimetry [35,36]. Despite the potential and growing interest in the EPID as an in vivo dosimeter, this method requires an extensive workload and software processing to be implemented. Considering lung SBRT VMAT delivery, there are only limited reported studies investigating the sensitivity of different dosimeters to intentionally introduced errors in multi-leaf collimator (MLC), gantry, collimator and dosimetric errors. Kim et al. [28] investigated the sensitivity of EBT2 films and MapCHECK to detect clinically unacceptable MLC misalignments. They found that MLC errors were detected using a 2%/1 mm global criterion while a 2%/2 mm criterion was not sufficiently sensitive. In our previous experimental study [37], we have studied the sensitivity of the ArcCHECK dosimeter to delivery errors in multi-leaf collimator (MLC), gantry, and collimator for Lung SBRT VMAT treatment plans. Not all deliberately introduced errors were detected using different gamma criteria of 1%/1 mm, 2%/1 mm, 2%/2 mm, and 3%/3 mm and this is possibly because of the detector resolution. Owing to the practicality and the high resolution of the EPID, the aim of this work is to study the sensitivity of an EPID in detecting delivery errors in the collimator angle, and MLC positions for VMAT lung stereotactic body radiotherapy (SBRT) using the Collapsed Arc method.

2. Materials and methods

2.1. VMAT SBRT planning and EPID dosimetric model

VMAT plans were generated for 15 lung cancer patients in a previous planning study [38]. Intentional errors were also introduced by modifying collimator angles by −5, −2, −1, +1, +2 or +5°and MLC field sizes (MLCFS) and MLC shifts (MLCShift) by −5, −2, −1, +1, +2 or +5 mm. Collimator and MLC errors were determined which caused any one or more of a range of DVH metrics to deviate by more than ± 2%. The DVH metrics included the following structures and parameters; PTV (D_{mean}, D_{max}, V95%, V100%), spinal cord (D_{mean}, D0.1 cc), and healthy lung (lung-PTV) (D_{mean}, V20Gy) [38]. The VMAT plans were based on RTOG0236 and RTOG0915 planning guidelines [39,40]. The plans were generated in Pinnacle (Phillips Healthcare, Fitchburg, WI, USA), v9.8 treatment planning system (TPS), using a 6 MV photon beam for an Elekta Versa HD linear accelerator with a 40 leaf pairs Agility MLC (Elekta, Crawley, UK). For all patients, the plan consisted of two 200-degree arcs with non-zero collimator angle to avoid doses due to interleaf leakage and to minimize tongue and groove effects. All lung SBRT VMAT baseline (no error) plans and error-introduced plans were exported to the Elekta Synergy Linac using the Mosaiq system (Elekta, Crawley, UK).

To calculate TPS planar dose matrices (fluence maps), each VMAT baseline plan was copied to a virtual water phantom by the TPS at 100 cm SAD and the plan was then collapsed to a single plane to produce a 2D TPS dose matrix in Pinnacle using the collapsed arc algorithm script. The collapsed arc method involves the calculation of the dose matrix in a plane perpendicular to the beam axis of the VMAT arc, this technique was validated by Nicolini et al. [41,42] for VMAT plans and is here used for the SBRT VMAT plans. The dose plane was extracted at depth d_{ref} = 5.4 cm. A dose grid size of 0.1 × 0.1 cm^2 was used in the dose map calculation to ensure sufficient resolution. This QA method used the EPID device to perform treatment dose verification and it was based on the approach primarily developed by Lee et al. [43] for IMRT verification using Varian EPID. The method was then extended by Tyler et al. [44] to include VMAT verification on different Linac's vendors and TPS including the Elekta EPID and Pinnacle TPS. The methodology was previously validated against a 2D ion chamber array [43,45] and has been used clinically in our center. Xing et al. [45] developed the software analysis to automate the process for our local implantation. This EPID model compared EPID images (EPID calibrated dose) and TPS dose fluence maps generated at pre-determined depth in water (d_{ref}). The reference depth in water was determined as the depth in water that had closest agreement to the dose response of the EPID [43,44]. The model has worked well for modulated treatment [43,44] but it has not been tested for Lung SBRT VMAT scenario.

2.2. Plan selection and the clinical significance of errors

The clinical significance and dosimetric impact of the delivery errors selected in this study were assessed in our previous planning study [38]. Different patients were found to have different sensitivity to the introduced errors. The smallest of the introduced errors resulting in ≥ ± 2% dose difference in any of the selected DVH metrics between the modified treatment plan compared to the baseline plan as shown in Table 1, together with baseline plans were delivered to an Elekta iViewGT EPID.

In the planning study [38], MLCFS errors were observed to have the highest impact on the DVH metrics. For this reason and following a similar approach to our previous experimental study using the ArcCheck detector [37], an additional group with larger MLCFS errors was selected. This included seven plans for +5 mm error, seven plans for +2 mm error, and two plans for −2mm.

2.3. Treatment delivery and EPID image acquisition

In this study, a total of 103 plans (in which 15 plans were baseline plans) were measured with the EPID while the gantry was rotated during acquisition and no phantom was present in the beam (non-transmission dosimetry). All measurements were carried out using an Elekta Synergy linear accelerator (Elekta, Crawley, UK) and an amorphous silicon EPID (Elekta iView GT). The Elekta EPID has a sensitive area of 41 cm × 41 cm in size and an effective source-detector distance of 160 cm [46,47]. Lung SABR VMAT EPID images were acquired for all baseline plans and error-introduced plans per individual arc (a total of 206 Arcs) with the iViewGT software using the 'multiple' exposure option. A 10x10 cm^2 static open beam calibration field (20 MU) using the 'single' exposure option was also measured over the period during which the measurements were performed. The EPID images and

Table 1
The plan number selected for each of the considered errors where that plan had the smallest error where a ± 2% dose deviation in any of the selected DVH metrics was seen, for the 15 Lung VMAT SBRT patient datasets.

Error type	Collimator (degree)				MLCShift (mm)					MLCFS (mm)	
Magnitude	+1	+5	−2	−5	+1	+2	+5	−1	−2	+1	−1
Number of selected plan	1	7	2	3	7	6	2	6	9	15	15

associated log files were exported from the iViewGT workstation for further analysis.

2.4. Dose matrix analysis

The measured EPID images were converted into dose matrices using existing methodology and Matlab computer code outlined elsewhere [45]. The EPID images were converted into dose matrices and calibrated to the dose at reference depth in water (d_{ref} = 5.4 cm) at an isocenter plane similar to the TPS dose matrices setup [43–45]. In this study, a unique approach was used to assess and verify sensitivity of the EPID to the introduced errors by making two dosimetric comparisons. Firstly, the error-introduced EPID measured dose matrices were compared to the baseline (no error) TPS matrices. This was done (EPID vs TPS) to give a measure of the sensitivity of this particular clinical EPID dosimetry model to the introduced delivery errors. Secondly, the error-introduced EPID measured dose matrices were compared to the baseline (no error) EPID measured dose matrices (EPID vs EPID) to give a measure of the raw sensitivity of the EPID. In each case, the error-introduced EPID measured dose matrices were compared to the baseline (no error) dose matrices using gamma (γ) analysis [48] as well as profile analysis in OmniPro I'mRT (IBA Dosimetry, V1.6) software. The gamma analysis was performed using global (G) dose and distance-to-agreement (DTA) tolerances with 1%/1 mm, 2%/1 mm, 2%/2 mm, and 3%/3 mm. The dose points receiving less than 10% of the maximum dose in the dose matrix were not considered in the analysis. The EPID images were left at their native resolution (0.0255 cm) when comparing EPID versus EPID and were interpolated to (0.1 cm) when compared to the TPS dose matrices.

3. Results

3.1. Comparison of the error-introduced EPID measured dose matrices versus TPS dose matrices

The resulting EPID measured dose and TPS dose matrices were compared using gamma analysis with different criteria. Table 2 shows the average (± 1SD) global gamma pass rates for the lung SBRT VMAT plans for no error (NE) and error-introduced plans. Overall, the majority of simulated errors were detected with gamma tolerance of 2%/1 mm and 1%/1 mm, and the gamma pass rates decreased as the magnitude of the error increased. The negative and positive MLC field size (± MLCFS) errors were the most detected errors across all error types. MLCShift errors of +1 mm and collimator errors of +1° and −2° were not detected for any of the considered gamma criteria, although 2%/1 mm and 1%/1 mm criteria showed slightly lower pass rate but not significant enough to discriminate those errors.

An example of the profile analysis for no error (NE) and error-introduced plans for lung SBRT VMAT is shown in Fig. 1 for collimator angle, MLCFS, and MLCShift error scenarios (Zoomed in images are shown in Appendix A; Figs. A1–A6). The profile analysis comparing EPID measured profiles and TPS calculated no error profiles, showed a clear effect of the introduced errors on the dose profile. By applying more stringent gamma criteria such as 2%/1 mm, and 1%/1 mm when analyzing the profile, the observed impact of the errors was more enhanced.

Table 2
Summary of the mean (± 1SD) global gamma pass rate for lung SABR VMAT plans measured on the EPID and delivered with different collimator, MLCFS and MLCShift errors. EPID measured error plans were compared to the no error (NE) TPS calculated plans. Each plan consisted of two Arcs (Arc1 and Arc2). A lower gamma pass rate number indicates greater sensitivity to error detection.

Plan Number	Error Type/Magnitude		Mean (± 1SD) global gamma pass rate (%)			
	No Error plan	Arc	3%/3 mm	2%/2 mm	2%/1mm	1%/1mm
15	NE1	Arc1	95.27 (3.4)	83.92 (5.1)	71.07 (4.7)	63.82 (5.5)
	NE2	Arc2	95.22 (2.0)	83.03 (3.7)	70.27 (4.7)	63.64 (5.1)
Error plans	Collimator (degree)					
1	+1°	Arc1	96.53	85.37	72.46	65.73
		Arc2	94.51	82.75	71.49	64.25
7	+5°	Arc1	94.05 (3.7)	82.21 (4.5)	68.84 (4.5)	61.88 (6.1)
		Arc2	94.55 (2.0)	82.26 (2.0)	68.90 (3.1)	62.17 (4.9)
2	−2°	Arc1	96.43 (2.9)	85.36 (4.6)	71.06 (3.8)	61.04 (6.5)
		Arc2	93.17 (1.9)	82.16 (0.75)	69.78 (5.6)	62.12 (6.3)
3	−5°	Arc1	93.42 (2.4)	79.29 (1.7)	66.03 (4.8)	59.87 (6.4)
		Arc2	91.42 (3.0)	78.32 (3.7)	66.42 (4.0)	59.63 (4.1)
MLCFS (mm)						
15	+1	Arc1	93.62 (4.3)	80.57 (5.2)	67.32 (5.8)	61.40 (7.1)
		Arc2	93.34 (3.0)	79.71 (5.9)	67.79 (6.8)	62.12 (7.2)
7	+2	Arc1	87.85 (6.7)	73.22 (6.6)	60.75 (7.4)	55.39 (7.5)
		Arc2	86.77 (6.3)	72.04 (8.0)	61.29 (8.0)	56.17 (8.0)
7	+5	Arc1	70.82 (7.9)	59.68 (8.8)	55.40 (9.6)	51.81 (8.5)
		Arc2	68.72 (8.8)	59.81 (8.3)	55.69 (8.6)	51.62 (7.3)
15	−1	Arc1	94.77 (3.5)	83.64 (4.7)	69.91 (5.3)	63.41 (6.2)
		Arc2	94.00 (3.8)	81.64 (5.3)	69.04 (5.3)	63.32 (5.7)
1	−2	Arc1	90.07	73.62	59.02	53.7
		Arc2	93.88	79.27	64.67	55.48
MLCShift (mm)						
7	+1	Arc1	94.48 (3.0)	83.22 (3.7)	70.04 (5.6)	63.41 (6.3)
		Arc2	94.28 (2.1)	83.73 (3.7)	70.06 (6.1)	63.07 (6.2)
6	+2	Arc1	92.20 (3.8)	76.30 (6.9)	64.26 (7.9)	59.35 (9.1)
		Arc2	94.10 (5.2)	81.52 (6.8)	66.95 (5.0)	61.09 (6.1)
2	+5	Arc1	77.39 (4.4)	68.09 (0.3)	62.68 (2.3)	60.32 (3.0)
		Arc2	70.37 (1.6)	64.34 (0.6)	60.96 (2.3)	59.13 (3.2)
6	−1	Arc1	94.35 (8.1)	82.43 (9.2)	68.92 (8.0)	62.92 (7.8)
		Arc2	91.88 (4.0)	78.47 (4.3)	68.05 (5.8)	62.59 (6.5)
9	−2	Arc1	89.31 (6.5)	74.39 (4.2)	64.74 (3.9)	60.18 (5.9)
		Arc2	87.19 (5.5)	72.66 (5.0)	64.35 (6.0)	60.19 (6.7)

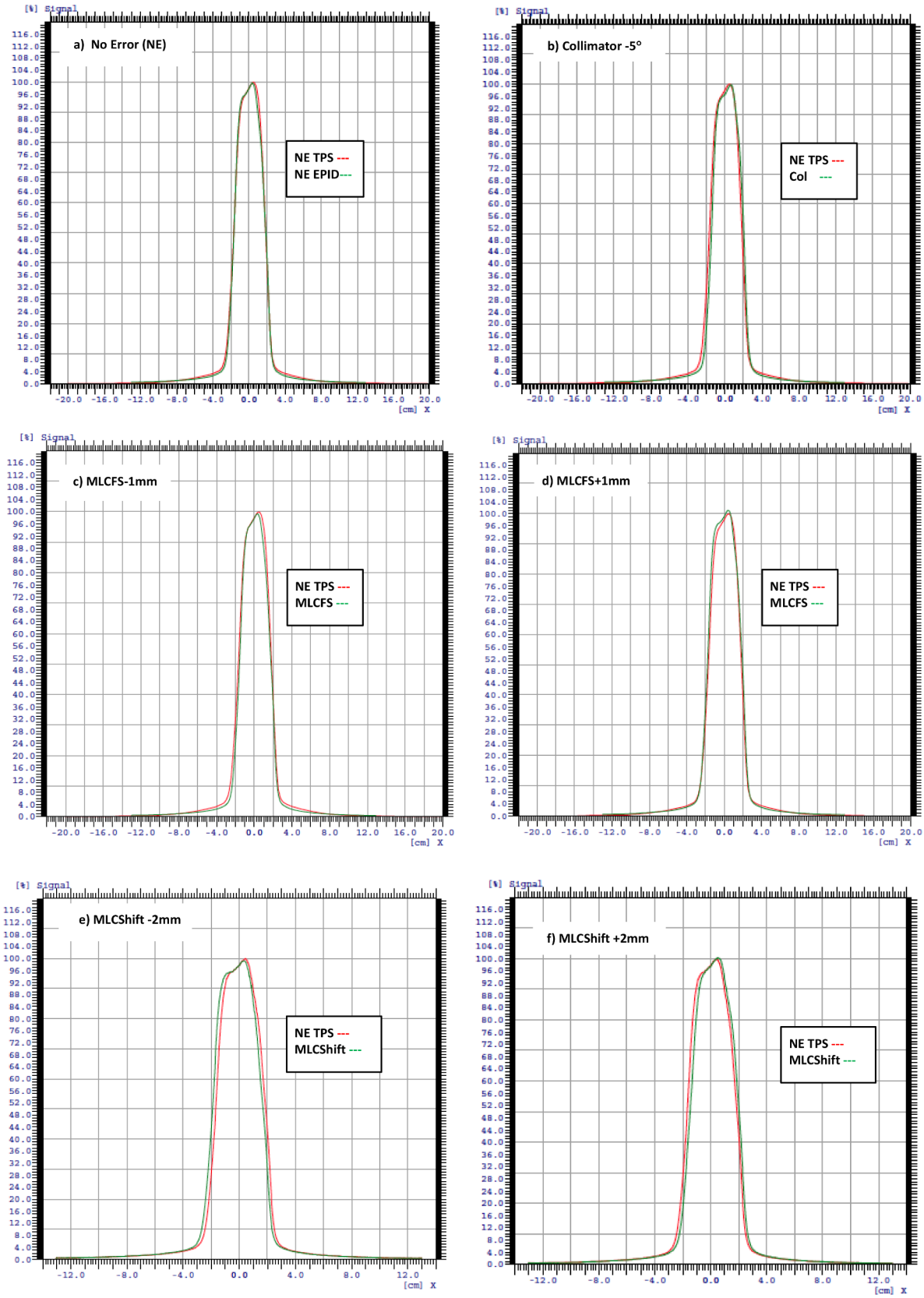

Fig. 1. Dose profile comparison between EPID measured dose (in green) and calculated TPS No Error (NE) plan (in red) with no error shown in (a) and with simulated errors including; (b) −5° Collimator, (c) −1 mm MLCFS, (d) +1 mm MLCFS, (e) −2 mm MLCShift and (f) +2 mm MLCShift errors. The effect of the errors was clearly seen on the profile and more pronounced effects were observed with larger error magnitudes. (patient 1 with the associated errors was selected here to give an example of the result).

3.2. Comparison of the error-introduced EPID measured dose matrices versus EPID measured no error (NE) dose matrices

Table 3 presents the average (± 1SD) global gamma pass rates for the error-introduced EPID measured dose matrices when compared to the EPID no error (NE) measured dose matrices. It can be seen that the general detection trend is relatively comparable to the previous results when comparing error-introduced EPID measured dose to the TPS calculated dose, in which collimator errors of +1 and −2° had no significant change in the gamma pass rate when compared to the no error plan for all gamma criteria. The correlation between the selected gamma tolerances and detected error magnitude was very clear based on the average gamma pass rate. For example, the rather loose 3%/3mm criteria could only detect a large MLC error of +5 mm, while the 2%/2mm criteria showed slightly better sensitivity to MLC error magnitude of ± 2 mm and collimator error of ± 5°. When using 2%/1mm criteria and 1%/1mm, all MLC errors (± 1, ± 2, +5mm) and ± 5-degree collimator errors were resolved with reasonable confidence as shown in Table 3.

Fig. 2 shows an example of the EPID measured dose matrices and the gamma map for different error types; collimator angle, ± MLCFS, and ± MLCShift compared to the EPID measured dose matrix for no error (NE) plan as a reference. It can also be noticed that the effect of all introduced errors was visible in the gamma map analysis with more sensitivity to the error depending on the gamma tolerances and the spatial resolution of the EPID.

4. Discussion

In this study, we presented and assessed a relatively simple method for pre-treatment verification of lung SBRT VMAT plans with different collimator and MLC errors. This method is easy to implement and does not require any sophisticated analytical or EPID modelling approaches. By using an EPID device and the collapsed arc technique, the majority of the errors were detected with sensitivity to errors depending on the gamma tolerances and the error magnitude. In general, we have found that the overall detection level was approximately similar when the error-introduced EPID measured dose matrices were compared to either calculated TPS or EPID measured dose for no error plans as shown in Tables 2 and 3. The EPID was able to quantify collimator error of ± 5° and the majority of MLCFS and MLCShift errors (± 2 and +5 mm) were resolved when using tighter gamma tolerance than 3%/3mm.

When the error-introduced EPID measured dose matrices were compared to TPS dose matrices, a substantial number of errors had a lower pass rate than no error plans and were detected when using different gamma criteria (Table 2). MLCFS errors which had the highest impact on the DVH metrics [38] were more resolved than other errors. The variation between different plan, as represented by (SD) that was seen in the gamma pass rates could be attributed to different factors such as; TPS calculation for both small field size and VMAT delivery, linac instability during gantry rotation, possible displacement of the EPID due to gravity. In addition, the selected plans in our study represent a sample of the typical clinical situations of lung SBRT VMAT

Table 3
Summary of the mean (± 1SD) global gamma pass rate for lung SABR VMAT plans measured on the EPID and delivered with different collimator, MLCFS and MLCShift errors. EPID measured error-introduced plans were compared to the no error EPID measured plans. Each plan consisted of two Arcs (Arc1 and Arc2). A lower gamma pass rate number indicates greater sensitivity to error detection.

Plan Number	Error Type/Magnitude	Mean (± 1SD) global gamma pass rate (%)				
			3%/3 mm	2%/2 mm	2%/1mm	1%/1mm
Collimator (degree)						
1	+1°	Arc1	100	100	99.98	99.66
		Arc2	100	100	100	99.67
7	+5°	Arc1	99.64 (0.7)	97.98 (2.5)	90.55 (5.2)	87.71 (6.2)
		Arc2	99.87 (0.2)	98.41 (2.1)	90.89 (4.3)	88.03 (5.6)
2	−2°	Arc1	100 (0)	100 (0)	98.92 (0.7)	98.08 (1.1)
		Arc2	100 (0)	100 (0)	99.56 (0.3)	98.97 (0.5)
3	−5°	Arc1	99.98 (0.03)	97.80 (2.0)	87.36 (4.4)	83.95 (5.8)
		Arc2	99.98 (0.03)	98.70 (1.1)	88.22 (3.7)	85.22 (5.0)
MLCFS (mm)						
15	+1	Arc1	99.94 (0.2)	99.95 (0.2)	97.03 (1.5)	92.747 (1.8)
		Arc2	99.99 (0.1)	99.98 (0.2)	98.44 (0.9)	94.19 (1.8)
7	+2	Arc1	99.89 (0.1)	97.61(1.0)	76.0 (4.1)	71.29 (4.9)
		Arc2	99.84 (0.3)	97.35 (2.2)	74.48 (4.8)	68.59 (6.6)
7	+5	Arc1	75.67 (3.7)	65.41 (5.1)	60.15 (7.1)	56.76 (7.3)
		Arc2	74.47 (4.5)	62.09 (7.3)	57.56 (8.7)	54.4 (7.5)
15	−1	Arc1	100 (0)	99.91 (0.2)	96.73 (1.4)	92.71 (2.2)
		Arc2	99.97 (0.1)	99.88 (0.2)	97.07 (2.5)	93.44 (3.2)
1	−2	Arc1	99.37	97.73	74.51	68.57
		Arc2	100	97.6	77.09	68.45
MLCShift (mm)						
7	+1	Arc1	100 (0)	100 (0)	96.27 (4.1)	92.24 (5.2)
		Arc2	100 (0)	100 (0)	97.73 (1.5)	93.06 (3.0)
6	+2	Arc1	100 (0)	96.98 (2.5)	75.78 (5.0)	71.89 (6.5)
		Arc2	100 (0)	98.86 (0.7)	76.15 (4.0)	71.64 (5.3)
2	+5	Arc1	76.0 (3.7)	68.60 (0.9)	65.34 (0.6)	63.65 (1.3)
		Arc2	75.51 (2.2)	68.95 (1.6)	65.73 (2.1)	63.37 (3.7)
6	−1	Arc1	100 (0)	100 (0)	96.95 (3.0)	92.97 (5.1)
		Arc2	100 (0)	100 (0)	98.13 (1.9)	93.61 (3.2)
9	−2	Arc1	100 (0)	95.68 (3.2)	75.91 (3.1)	72.30 (4.1)
		Arc2	100 (0)	95.87 (2.3)	75.51 (3.1)	71.56 (4.5)

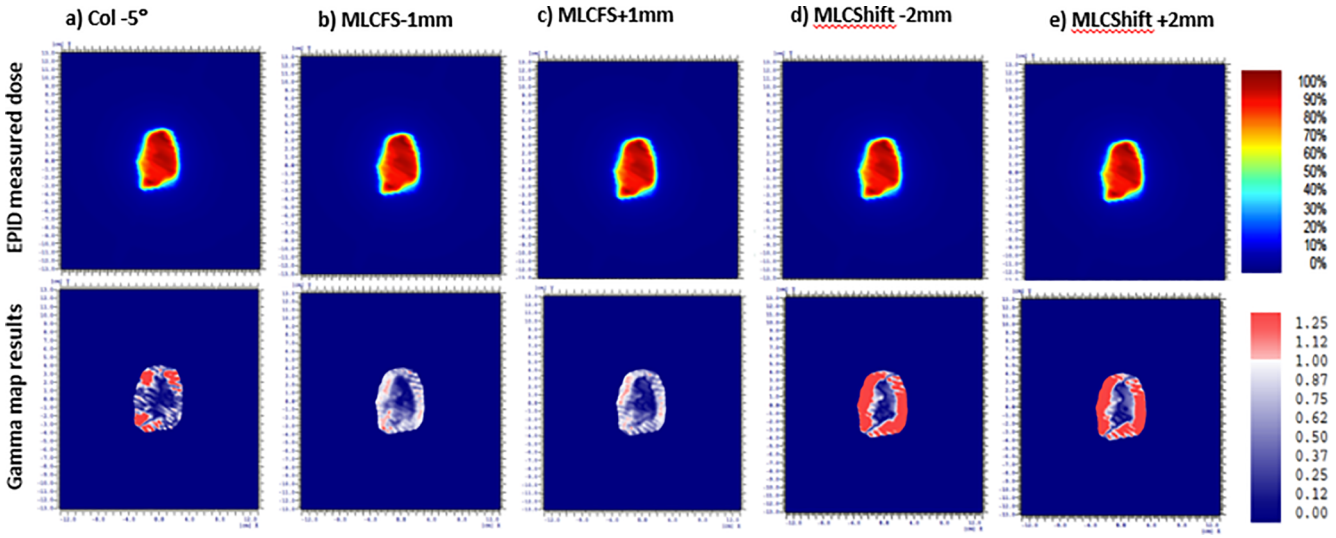

Fig. 2. An example of EPID measured dose matrices for different error types; (a) collimator angle, (b, c) ± MLCFS, and (d, e) ± MLCShift. The top row is for the purpose of demonstrating location of the error in the bottom row. The resulting gamma map when comparing the error-introduced EPID measured dose matrices for those errors to the EPID measured dose matrix for no error (NE) plan as a reference (bottom row). (patient 1 with the associated errors producing clinically significant changes in plan metrics was selected here to give an example of the result).

plans in which the prescribed dose and the patient cohort were classified into three categories according to the physical location of the primary tumor [38]. This may also have an impact on the average gamma pass rate.

Zhu et al. [20] in their study comparing VMAT dosimetric verifications between rotating and fixed (collapsed arc delivered at 0°) gantry, found that the gamma pass rate decreased by about 6% for rotation delivery using 2%/2mm criteria. They investigated different dosimeters including EPID and compared measured and TPS calculated dose using different gamma criteria. Moreover, a further study on using the EPID for an in vivo dose verification method for lung SBRT VMAT delivery showed that a 2%/2mm criteria resulted in an average gamma pass rate of 88% which is relatively comparable to our result [35]. Kim et al. [28] recommended 2%/1mm criteria to be used to evaluate VMAT plans for SBRT techniques. In agreement with Kim et al. 2%/1mm criteria was able to resolve more errors in the current study than any other criteria with reasonable average pass rate as shown in Table 2. The use of 1%/1mm in this study was just to see what is the minimum error that could be detected for all error scenarios. Previous studies did not recommend the use of 1%/1mm gamma criteria and reported that it is more susceptible to statistical fluctuations [49,50].

Some examples of the collimator, MLCFS and MLCShift errors were further assessed in the profile analysis as shown in Fig. 1 (see also Appendix A; Figs. A1–A6 for the zoomed images). All the MLC errors types and ± 5° collimator errors were visually resolved when compared to the no error TPS profiles. The effect of the introduced-errors was more clear in the profile analysis particularly for larger error magnitude. Fig. 1 illustrates profile analysis utilizing 2%/1mm gamma criteria for patient one in this study with the relevant selected errors producing clinically significant changes in plan metrics at levels previously described (Section 2.1 and Ref. [39]).

Because treatment delivery and planning are never perfect and to further assess the raw sensitivity of the EPID to delivery errors using the collapsed arc method, the error-introduced EPID measured dose matrices were compared to the EPID measured no error (NE) dose matrices. Generally, the sensitivity of the EPID in detecting the errors were significantly depending on the gamma tolerance setting and more errors were detected with tighter gamma criteria as shown in Table 3. The EPID was able to resolve ± 5° collimator errors and all the MLCFS and MLCShift errors, with average gamma pass rates dropping with increased error magnitude. 2%/1 and 1%1mm gamma tolerance were able to quantify all the errors with sufficient confidence. These results which were presented in an ideal case here may help to understand which criteria are needed to detect a specific error magnitude with an EPID device for a specific treatment technique. In Fig. 2, examples are given of the EPID measured dose matrices for the error plans and the resulting gamma map when compared to no error EPID measured dose matrices using criteria of 2%/1mm for the same patient as in the previous section. Even the effect of a smaller MLCFS error (± 1 mm) were visible in the gamma map analysis with slightly higher pass rate than other error magnitudes as seen from Table 3.

It is very clear that, as expected, all the fails were in the field edge (penumbra) region as shown in Figs. 1 and 2. It is also obvious that the lung SBRT fields are less complex and not very modulated compared to H&N and prostate plans. As a result, the integrated EPID images looks similar to an open field. Therefore, depending perhaps on target size, the high dose gradients will be predominantly in the field penumbra and distance to agreement error is likely to dominate the gamma result around the field edges. This is important in lung SBRT where the minimum dose to the target will drop dramatically with geometric errors. Low resolution detectors could pick up dose differences but can miss distance to agreement errors, and therefore be less appropriate for these lung SBRT scenarios. In comparison with our previous study [37] using the ArcCheck detector for the same data set, the ArcCheck was not able to detect most of the positive MLCShift errors and some of the negative MLCShift and MLC field size errors. It failed also to resolve the majority of the collimator errors. In addition, the gamma pass rate showed a considerable variation. In agreement with previous studies, Woon et al. [27] demonstrated that low resolution detectors such as ArcCheck can affect gamma pass rates and fail to accurately detect MLC errors. Bruschi et al. [26] also found that the detector resolution has a significant impact on the pre-treatment verification of SBRT plans. Overall, this EPID evaluation method seems to be more sensitive than other methods and the correlation between the selected gamma tolerances and detected error magnitude was clearly demonstrated based on the average gamma pass rate.

This work demonstrated the feasibility and effectiveness of a relatively simple method using the collapsed arc technique and EPID for pre-treatment verification of lung SBRT VMAT plans. One of the advantages of EPIDs over other types of dosimeters for lung SBRT verification is that EPID dosimeters have high spatial resolution; and thus enable accurate detection of the errors and a robust verification of dose

for the VMAT approach [43]. However, as the EPID measurement plane is always perpendicular to the gantry, the Collapsed Arc technique is unable to detect any possible gantry delivery errors.

Future work including a gantry inclinometer during the measurement or acquiring the EPID images in a continuous mode to convert each frame individually may provide improved tools and feedback to detect such potential errors. Once the EPID is calibrated for dosimetry and the radiotherapy system is verified by appropriate commissioning tests (including delivery and TPS), the method presented in this work appears to be suitable for pre-treatment patient QA of lung SBRT VMAT plans. The results presented in this work are specific to the EPID dosimetry model used here and further work needs to be done to extend them to other EPID dosimetry model implementations.

5. Conclusion

This work showed the feasibility and effectiveness of a relatively simple method using the collapsed arc technique and aSi-EPID for pre-treatment verification of lung SBRT VMAT plans. The EPID was able to detect the majority of MLCFS, MLCShift and collimator errors with specific sensitivity to errors depending on the gamma tolerances used. Adoption of tighter gamma tolerances improved the resolution of more errors and the 2%/1mm criteria showed higher sensitivity to the introduced errors for this group of patients.

Appendix (A)

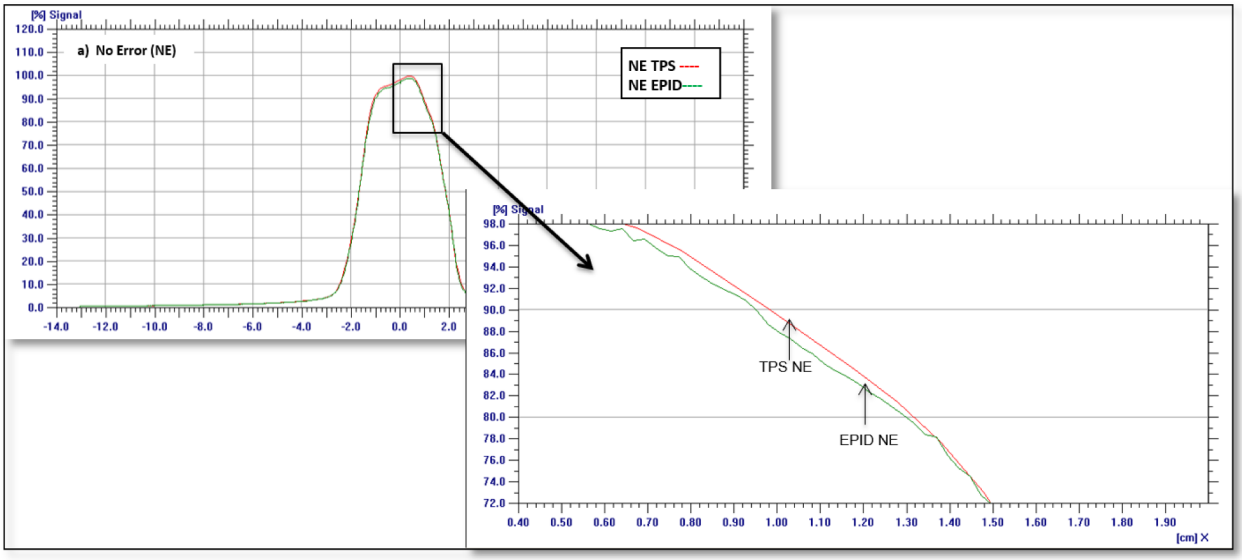

Fig. A1. Zoomed in image of Fig. 1.a) showing dose profile comparison between No Error (NE) EPID measured dose (in green) and calculated TPS for No Error (NE) plan (in red).

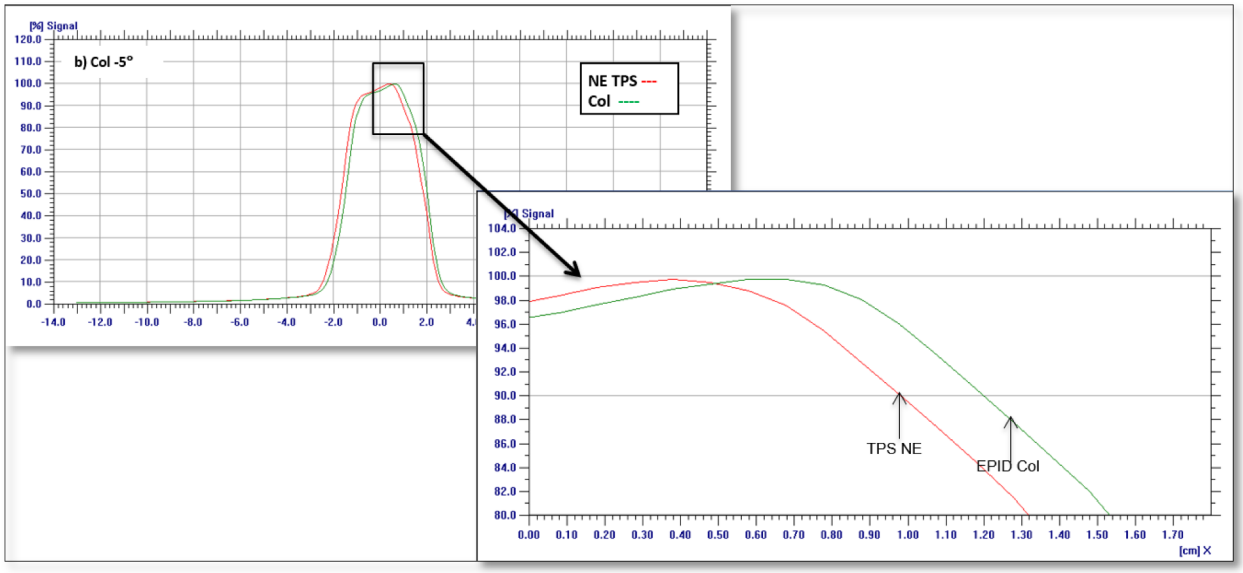

Fig. A2. Zoomed in image of Fig. 1.b) showing dose profile comparison between EPID measured dose with −5° collimator simulated error (in green) and calculated TPS dose for No Error (NE) plan (in red).

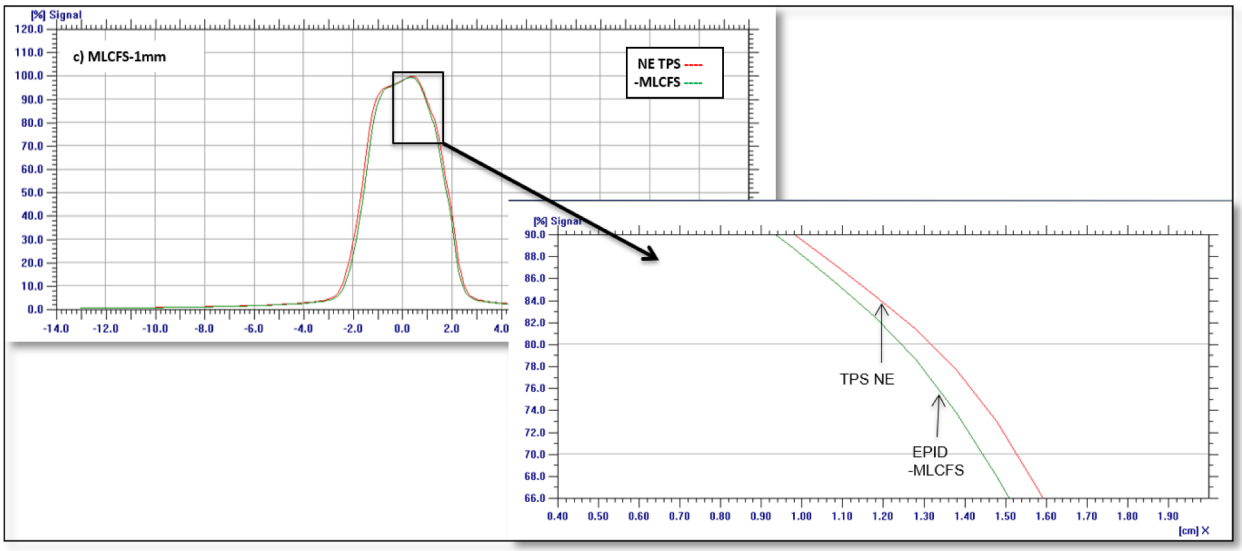

Fig. A3. Zoomed in image of Fig. 1.c) showing dose profile comparison between EPID measured dose with −1 mm MLCFS simulated error (in green) and calculated TPS dose for No Error (NE) plan (in red).

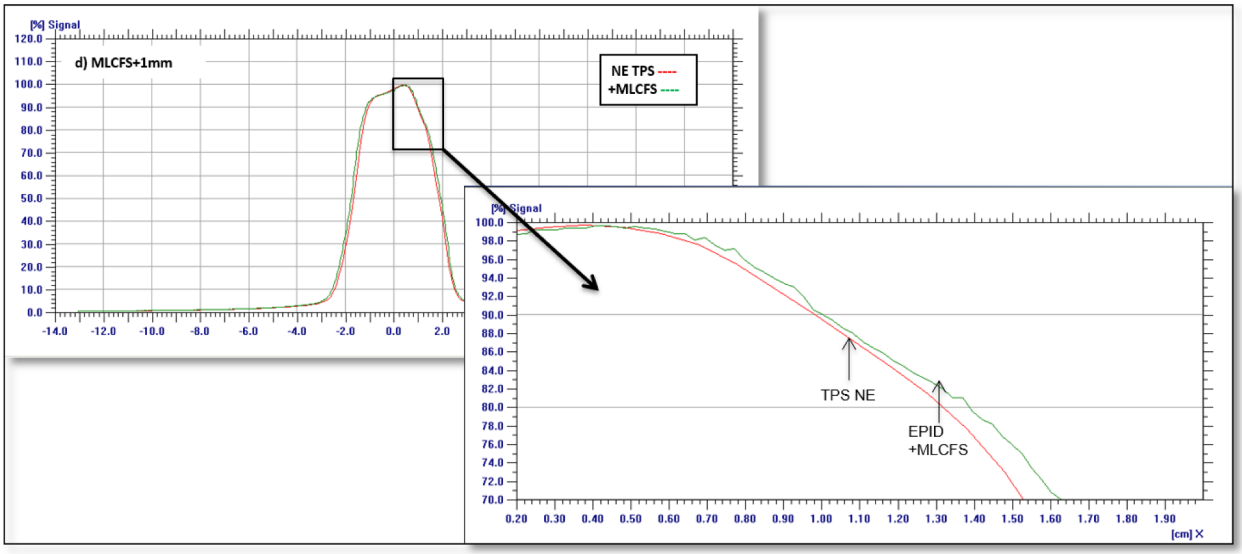

Fig. A4. Zoomed in image of Fig. 1.d) showing dose profile comparison between EPID measured dose for with + 1 mm MLCFS simulated error (in green) and calculated TPS dose for No Error (NE) plan (in red).

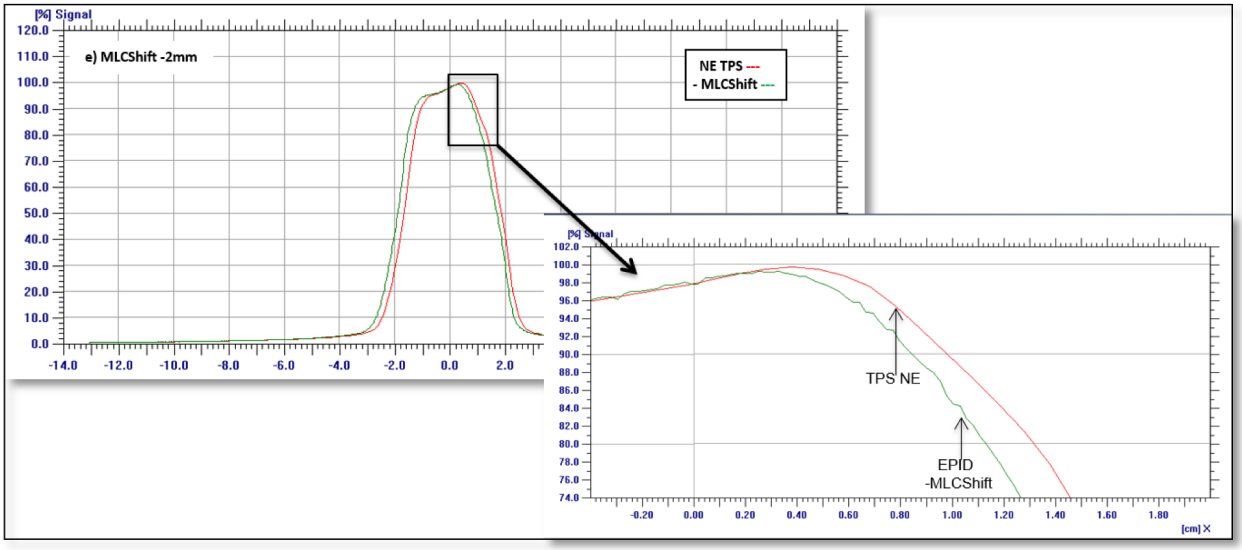

Fig. A5. Zoomed in image of Fig. 1.e) showing dose profile comparison between EPID measured dose with −2mm MLC Shift simulated error (in green) and calculated TPS dose for No Error (NE) plan (in red).

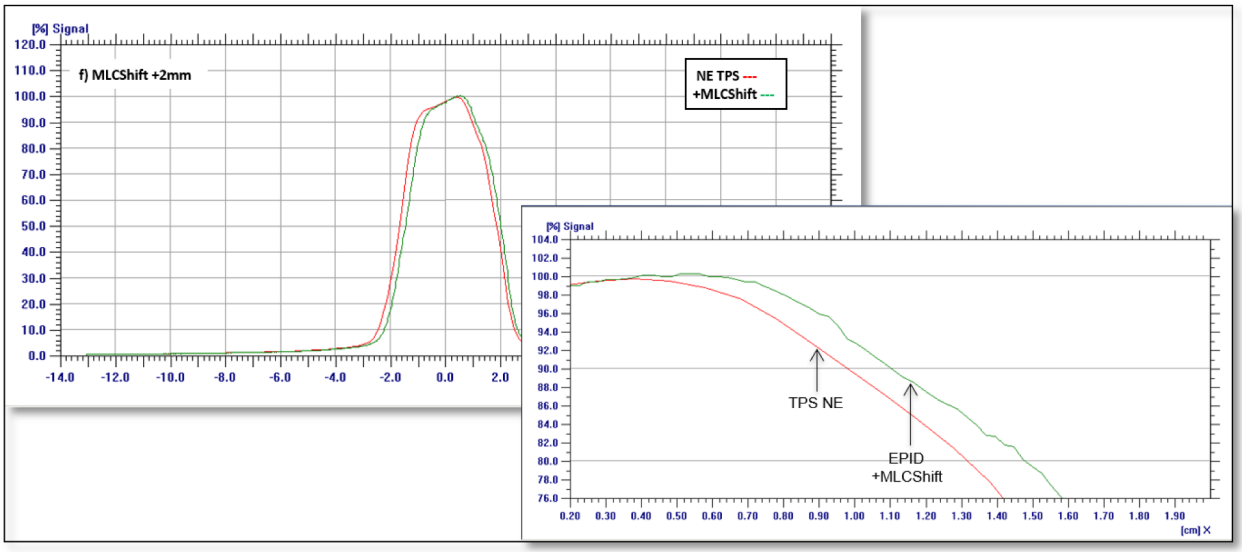

Fig. A6. Zoomed in image of Fig. 1.f) showing dose profile comparison between EPID measured dose with + 2 mm MLC Shift simulated error (in green) and calculated TPS dose for No Error (NE) plan (in red).

References

[1] Otto K. Volumetric modulated arc therapy: IMRT in a single gantry arc. Med Phys 2008;35(1):310–7.
[2] Webb S, McQuaid D. Some considerations concerning volume-modulated arc therapy: a stepping stone towards a general theory. Phys Med Biol 2009;54(14):4345.
[3] Schreibmann E, Dhabaan A, Elder E, Fox T. Patient-specific quality assurance method for VMAT treatment delivery. Med Phys 2009;36(10):4530–5.
[4] O'Daniel J, Das S, Wu QJ, Yin FF. Volumetric-modulated arc therapy: effective and efficient end-to-end patient-specific quality assurance. Int J Radiat Oncol Biol Phys 2012;82(5):1567–74.
[5] Kestin L, Grills I, Guckenberger M, Belderbos J, Hope AJ, Werner-Wasik M, et al. Dose–response relationship with clinical outcome for lung stereotactic body radiotherapy (SBRT) delivered via online imageguidance. Radiother Oncol 2014;110(3):499–504.
[6] Benedict SH, Yenice KM, Followill D, Galvin JM, Hinson W, Kavanagh B, et al. Stereotactic body radiation therapy: the report of AAPM Task Group 101. Med Phys 2010;37(8):4078–101.
[7] Giglioli FR, Clemente S, Esposito M, Fiandra C, Marino C, Russo S, et al. Frontiers in planning optimization for lung SBRT. Physica Med 2017;44:163–70.
[8] Pallotta S, Marrazzo L, Bucciolini M. Design and implementation of a water phantom for IMRT, arc therapy, and tomotherapy dose distribution measurements. Med Phys 2007;34(10):3724–31.
[9] Van Esch A, Clermont C, Devillers M, Iori M, Huyskens DP. On-line quality assurance of rotational radiotherapy treatment delivery by means of a 2D ion chamber array and the Octavius phantom. Med Phys 2007;34(10):3825–37.
[10] Spezi E, Angelini AL, Romani F, Ferri A. Characterization of a 2D ion chamber array for the verification of radiotherapy treatments. Phys Med Biol 2005;50(14):3361–73.
[11] Feygelman V, Zhang G, Stevens C, Nelms BE. Evaluation of a new VMAT QA device, or the"X" and "O" array geometries. J Appl Clin Med Phys 2011;12(2):3346.
[12] Bedford JL, Lee YK, Wai P, South CP, Warrington AP. Evaluation of the Delta4 phantom for IMRT and VMAT verification. Phys Med Biol 2009;54(9):N167.
[13] Vergote K, De Deene Y, Duthoy W, De Gersem W, De Neve W, Achten E, et al. Validation and application of polymer gel dosimetry for the dose verification of an intensity modulated arc therapy (IMAT) treatment. Phys Med Biol 2004;49(2):287–305.
[14] Bakhtiari M, Kumaraswamy L, Bailey DW, de Boer S, Malhotra HK, Podgorsak MB.

Using an EPID for patient-specific VMAT quality assurance. Med Phys 2011;38(3):1366–73.
[15] Bedford JL, Warrington AP. Commissioning of volumetric modulated arc therapy (VMAT). Int J Radiat Oncol Biol Phys 2009;73(2):537–45.
[16] Mans A, Remeijer P, Olaciregui-Ruiz I, Wendling M, Sonke J-J, Mijnheer B, et al. 3D dosimetric verification of volumetric-modulated arc therapy by portal dosimetry. Radiother Oncol 2010;94(2):181–7.
[17] Masi L, Casamassima F, Doro R, Francescon P. Quality assurance of volumetric modulated arc therapy: evaluation and comparison of different dosimetric systems. Med Phys 2011;38(2):612–21.
[18] Van Elmpt W, McDermott L, Nijsten S, Wendling M, Lambin P, Mijnheer B. A literature review of electronic portal imaging for radiotherapy dosimetry. Radiother Oncol 2008;88(3):289–309.
[19] Woodruff HC, Fuangrod T, Rowshanfarzad P, McCurdy B, Greer PB. Gantry-angle resolved VMAT pretreatment verification using EPID image prediction. Med Phys 2013;40(8).
[20] Zhu J, Chen L, Jin G, Luo G, Cao W, Liu X. A comparison of VMAT dosimetric verifications between fixed and rotating gantry positions. Phys Med Biol 2013;58(5):1315.
[21] Greer PB. 3D EPID based dosimetry for pre-treatment verification of VMAT–methods and challenges. Int J Phys Conf Ser 2013;444:012010.
[22] Mijnheer BJ, González P, Olaciregui-Ruiz I, Rozendaal RA, van Herk M, Mans A. Overview of 3-year experience with large-scale electronic portal imaging device–-based 3-dimensional transit dosimetry. Pract Radiat Oncol 2015;5(6):e679–87.
[23] Nelms BE, Chan MF, Jarry G, Lemire M, Lowden J, Hampton C, et al. Evaluating IMRT and VMAT dose accuracy: practical examples of failure to detect systematic errors when applying a commonly used metric and action levels. Med Phys 2013;40(11).
[24] Mans A, Wendling M, McDermott LN, Sonke JJ, Tielenburg R, Vijlbrief R, et al. Catching errors with in vivo EPID dosimetry. Med Phys 2010;37(6Part2):2638–44.
[25] Agnew A, Agnew CE, Grattan MW, Hounsell AR, McGarry CK. Monitoring daily MLC positional errors using trajectory log files and EPID measurements for IMRT and VMAT deliveries. Phys Med Biol 2014;59(9):N49.
[26] Bruschi A, Esposito M, Pini S, Ghirelli A, Zatelli G, Russo S. How the detector resolution affects the clinical significance of SBRT pre-treatment quality assurance results. Physica Med 2018;49:129–34.
[27] Woon W, Ravindran PB, Ekayanake P, Lim YY, Khalid J. A study on the effect of detector resolution on gamma index passing rate for VMAT and IMRT QA. J Appl Clin Med Phys 2018;19(2):230–48.
[28] Kim JI, Park SY, Kim HJ, Kim JH, Ye SJ, Park JM. The sensitivity of gamma-index method to the positioning errors of high-definition MLC in patient-specific VMAT QA for SBRT. Radiat Oncol 2014;28(9):167.
[29] Yang K, Yan D, Tyagi N. Sensitivity analysis of physics and planning SmartArc parameters for single and partial arc VMAT planning. J Appl Clin Med Phys 2012;13(6):34–45.
[30] Stambaugh C, Nelms BE, Dilling T, Stevens C, Latifi K, Zhang G, et al. Experimentally studied dynamic dose interplay does not meaningfully affect target dose in VMAT SBRT lung treatments. Med Phys 2013;40(9).
[31] Matuszak M, Yan D, Grills I, Martinez A. Volumetric modulated arc therapy for stereotactic body radiation therapy: initial clinical experience. Int J Radiat Oncol Biol Phys 2009;75(3):723–4.
[32] Hansen CR, Bertelsen A, Riis HL, Christiansen RL, Hansen O, Sykes JB, et al. Plan quality and delivery accuracy of flattening filter free beam for SBRT lung treatments. Acta Oncol 2015;54(3):422–7.
[33] Olding T, Alexander KM, Jechel C, Nasr AT, Joshi C. Delivery validation of VMAT stereotactic ablative body radiotherapy at commissioning. J Phys Conf Ser 2015;573:012019.
[34] Tyagi N, Yang K, Yan D. Comparing measurement-derived (3DVH) and machine log file-derived dose reconstruction methods for VMAT QA in patient geometries. J Appl Clin Med Phys 2014;15(4):4645.
[35] McCowan PM, Van Uytven E, Van Beek T, Asuni G, McCurdy BM. An in vivo dose verification method for SBRT–VMAT delivery using the EPID. Med Phys 2015;42(12):6955–63.
[36] Consorti R, Fidanzio A, Brainovich V, Mangiacotti F, De Spirito M, Mirri MA, et al. EPID-based in vivo dosimetry for stereotactic body radiotherapy of non-small cell lung tumors: initial clinical experience. Physica Med 2017;42:157–61.
[37] Alharthi T, Pogson EM, Arumugam S, Holloway L, Thwaites D. Pre-treatment verification of lung SBRT VMAT plans with delivery errors: toward a better understanding of the gamma index analysis. Physica Med 2018;49:119–28.
[38] Blake SJ, Arumugam S, Holloway L, Vinod S, Ochoa C, Phan P, et al. Investigating the impact of treatment delivery uncertainties on treatment effectiveness for lung SABR. Aust Phys Eng Sci Med 2017;40(4):823–9.
[39] Timmerman RD, Michalski J, Galvin J, Fowler JF, Choy H, Gore E, et al. R0236: a phase II trial of stereotactic body radiation therapy (SBRT) in the treatment of patients with medically inoperable stage I/II non-small cell lung cancer. Proceedings of the 13th World Conference on Lung Cancer. 2007.
[40] Videtic GM, Hu C, Singh AK, Chang JY, Parker W, Olivier KR, et al. A randomized phase 2 study comparing 2 stereotactic body radiation therapy schedules for medically inoperable patients with stage I peripheral non-small cell lung cancer: NRG Oncology RTOG 0915 (NCCTG N0927). Int J Radiat Oncol Biol Phys 2015;93(4):757–64.
[41] Nicolini G, Vanetti E, Clivio A, Fogliata A, Korreman S, Bocanek J, et al. The GLAaS algorithm for portal dosimetry and quality assurance of RapidArc, an intensity modulated rotational therapy. Radiat Oncol 2008;3(1):24.
[42] Nicolini G, Clivio A, Fogliata A, Vanetti E, Cozzi L. Simultaneous integrated boost radiotherapy for bilateral breast: a treatment planning and dosimetric comparison for volumetric modulated arc and fixed field intensity modulated therapy. Radiat Oncol 2009;4(1):27.
[43] Lee C, Menk F, Cadman P, Greer PB. A simple approach to using an amorphous silicon EPID to verify IMRT planar dose maps. Med Phys 2009;36(3):984–92.
[44] Tyler M, Vial P, Metcalfe P, Downes S. Clinical validation of an in-house EPID dosimetry system for IMRT QA at the Prince of Wales Hospital. Int J Phys Conf Ser 2013;444:012043.
[45] Xing A, Arumugam S, Deshpande S, Armia G, Holloway L, Goozee G, et al. Streamlining EPID-based IMRT quality assurance: auto-analysis and auto-report generation. Int J Phys Conf Ser 2014;489:012084.
[46] McDermott LN, Louwe RJ, Sonke JJ, Van Herk MB, Mijnheer BJ. Dose–response and ghosting effects of an amorphous silicon electronic portal imaging device. Med Phys 2004;31(2):285–95.
[47] Winkler P, Hefner A, Georg D. Dose-response characteristics of an amorphous silicon EPID. Med Phys 2005;32(10):3095–105.
[48] Low DA, Dempsey JF. Evaluation of the gamma dose distribution comparison method. Med Phys 2003;30(9):2455–64.
[49] Heilemann G, Poppe B, Laub W. On the sensitivity of common gamma-index evaluation methods to MLC misalignments in Rapidarc quality assurance. Med Phys 2013;40(3).
[50] Poppe B, Blechschmidt A, Djouguela A, Kollhoff R, Rubach A, Willborn KC, et al. Two-dimensional ionization chamber arrays for IMRT plan verification. Med Phys 2006;33(4):1005–15.